Single-Cell and Single-Molecule Analysis of Gene Expression Regulation

Maria Vera[1], **Jeetayu Biswas**[1,†], **Adrien Senecal**[1,†], **Robert H. Singer**[1,2], and **Hye Yoon Park**[3,4]

Maria Vera: maria.vera@einstein.yu.edu; Jeetayu Biswas: jeetayu.biswas@med.einstein.yu.edu; Adrien Senecal: adrien.senecal@einstein.yu.edu; Robert H. Singer: robert.singer@einstein.yu.edu; Hye Yoon Park: hyeyoon.park@snu.ac.kr

[1]Department of Anatomy and Structural Biology, Albert Einstein College of Medicine, New York, NY 10461

[2]Janelia Research Campus of the HHMI, Ashburn, Virginia 20147

[3]Department of Physics and Astronomy, Seoul National University, Seoul, 08826, Korea

[4]Institute of Molecular Biology and Genetics, Seoul National University, Seoul, 08826, Korea

Abstract

Recent advancements in single-cell and single-molecule imaging technologies have resolved biological processes in time and space that are fundamental to understanding the regulation of gene expression. Observations of single-molecule events in their cellular context have revealed highly dynamic aspects of transcriptional and post-transcriptional control in eukaryotic cells. This approach can relate transcription with mRNA abundance and lifetimes. Another key aspect of single-cell analysis is the cell-to-cell variability among populations of cells. Definition of heterogeneity has revealed stochastic processes, determined characteristics of under-represented cell types or transitional states, and integrated cellular behaviors in the context of multicellular organisms. In this review, we discuss novel aspects of gene expression of eukaryotic cells and multicellular organisms revealed by the latest advances in single-cell and single-molecule imaging technology.

Introduction

Conventional biochemical and molecular assays determine average properties of cell populations at single time points. These ensemble measurements have been extensively used to define gene expression patterns, signaling networks, and gene regulatory circuits. These methods, although useful, have established models of gene expression regulation that are being questioned by single-cell studies. This challenge originates from the fact that the information obtained from a population that characterizes the average cell does not represent

disclosure statement

The authors are not aware of any affiliations, memberships, funding, or financial holdings that might be perceived as affecting the objectivity of this review.

gene expression in single cells (80, 86). Variations among isogenic cells were first described in β-galactosidase expression in response to lactose induction (110). Single-cell studies have since revealed that cell heterogeneity rules most physiological processes and enables population survival (87). Hence, cell-to-cell variability provides a pathway to address the dynamic molecular mechanisms that individual cells use to function and adapt to the environment. Further development of technologies to quantify and follow single-mRNA and protein molecules is still required. For instance, cellular heterogeneity increases the complexity of modeling gene regulation in metazoans where cell differentiation assures organism survival. For these reasons, this review focuses on eukaryotic cells to discuss the latest advances in single-cell and single-molecule technologies.

The single-cell field arose from the development of three different methodologies: flow cytometry/fluorescence-activated cell sorting (FACS), single-cell RNA sequencing, and fluorescence microscopy. FACS is useful to catalog cell types based on the combination of protein markers (5). Although, FACS is still limited by the requirement of having antibodies to the target protein and does not provide information on gene expression regulation, the CRISPR (clustered regularly interspaced short palindromic repeats)-Cas technology overcomes this limitation by tagging specific endogenous genes with fluorescent proteins and aptamers that make the RNA recognizable (108, 129). Single-cell RNA sequencing provides a snapshot of the total cellular content of RNAs. This approach was incentivized by the central role of mRNA as a surrogate for gene expression and the technology to amplify single-mRNA molecules (158). Although RNA sequencing provides information on the whole-cell transcriptome and allows comparison of individual cells, the spatial information of the molecules in their cell microenvironment is lost during the process of single-cell separation.

Information on spatial position can be obtained by directly imaging the cells inside their native environment. The capabilities of fluorescence microscopy in analyzing gene expression have been empowered by the technologies that allow single-particle visualization. The central role of mRNA on gene expression regulation and the possibility of multiplexing complementary labeled oligos have made RNA the first molecule to reach the single-molecule resolution and to be quantified and localized within the fixed cells (50). In addition to the previously observed cell-to-cell variability with other technologies, single-molecule fluorescence in situ hybridization (smFISH) provides additional information on mRNA metabolism: It associates single-mRNA molecules with specific events, such as active transcription and nuclear export, and, therefore, models of gene expression regulation can be assessed (50). Development of the genetically encoded MS2 and PP7 orthologous systems has brought the time dimension into the field (11, 27). The metabolism of mRNA can be quantified to reveal dynamics of transcription, nuclear export, migration, and translation, and it can be used to build models of expression and decipher novel mechanisms at the level of a single cell. The understanding of these processes has been recently enriched with the ability to visualize single proteins (29, 139) and to resolve the dynamics and localization of single mRNAs as they are being translated in live cells (103, 150, 155, 157). The development of the super-resolution and other powerful microscopy techniques together with analytical tools to quantify, register, and track single molecules offers a new perspective to analyze gene

expression. These fixed and live approaches complement each other and have been made possible through the joint efforts of biologists, computer scientists, and physicists.

This review describes the available imaging technologies and how they have been used to understand transcriptional regulation and mRNA processing, localization, translation, and decay. Additionally, the perspectives gained from single-cell studies and their impacts on understanding multicellular organisms' biogenesis are discussed.

TECHNIQUES TO ANALYZE SINGLE-CELL AND SINGLE-MOLECULE EXPRESSION

Fluorescence microscopy is a widely used method for single-cell analysis in fixed and live cells because of its multiple advantages. First, the specificity of antibody- or nucleic acid–conjugated probes and genetically encoded fluorescent proteins enables highly selective detection of target molecules inside a cell. Second, there are a wide variety of fluorochromes, which allow multiplexed detection of several targets in a single assay. Third, quantitative analysis can be performed on digital images to determine the spatial and intensity information from fluorescence signals. Finally, live-cell imaging is possible because fluorescence signals can be collected with high sensitivity in real time.

Single-molecule resolution has been achieved by advances in microscopy techniques as well as labeling methods that amplify the signal emitted from individual molecules of RNA or protein. The development of super-resolution light microcopy, photo-activated localization microscopy (PALM), and stochastic optical reconstruction microscopy (STORM) (12, 67, 122) is based on the use of photo-switchable fluorescent probes to resolve multiple molecules located within a diffraction-limited spot. These and other imaging technologies have been extensively reviewed (92, 112) and are summarized in Table 1. This section explains tools designed to visualize single RNAs and proteins as well as technical developments to analyze them in fixed or live samples.

Snapshot Approaches to Single-Cell Analysis

The rationale for imaging is to obtain information on the spatial position of cellular components inside their native environment. Immunostaining and in situ hybridization have long been used for studying gene expression in the context of tissue structures. Single-mRNA molecules are detected in fixed cells by smFISH (50, 121) (Figure 1*a*). By hybridizing each mRNA with multiple probes labeled with fluorescent dyes, it is possible to detect single-mRNA molecules and count their number (Figure 2*a*). Variations of smFISH have been developed using 50-mer (50) or 20-mer (121) oligodeoxynucleotides (ODNs), branched DNA (bDNA) probes (6), and sequential tethered and intertwined ODN complexes (FISH-STICs) (131). In addition, specific protocols have been optimized for rapid diagnostics (128) and for detecting transcribed gene fusions (125), single-nucleotide variants (SNVs) (84), noncoding RNAs (21), and nascent mRNAs (85). Analysis of the image obtained by smFISH requires software, such as Localize and Air-Localize (89, 142, 159) or FISH-QUANT (104), to automatically count the number of transcripts in the nucleus and the cytoplasm and to quantify nascent mRNAs at active transcription sites (TSs) in three

dimensions. The relationship of the mRNA counts with their cellular distribution provides valuable information on mRNA retention in the nucleus (2, 7), mRNA half-life (144), and transcriptional output (69, 159).

Although smFISH provides extensive information on the metabolism of mRNA, it can assess only a few genes at a time. To overcome this limitation, a combinatorial probe labeling approach has been introduced to visualize 11 mRNAs simultaneously for multiplexed gene expression profiling (86). This approach has been combined with super-resolution microscopy (95), sequential probe hybridization and stripping (96), and a Hamming algorithm (30) to further increase the number of genes, potentially up to a thousand RNA species, for simultaneous detection. Moreover, fluorescence in situ RNA sequencing (FISSEQ) allows transcriptome sequencing by oligonucleotide ligation and detection (SOLiD) of reverse-transcribed cDNA inside cells (82). Although the current form of FISSEQ produces many fewer reads than RNA sequencing and is less accessible to genes involved in RNA and protein processing, it has potential for measuring transcriptomes in single cells within their spatial context.

Overall, smFISH provides accurate information on the number and localization of single-mRNA molecules. Quantification of large numbers of cells informs cell-to-cell variability, and the application of algorithms, such as FISH-QUANT, infers gene expression dynamics. Nonetheless, it lacks the capacity to follow the same particle over time, necessitating the development of live imaging of single molecules.

Real-Time Approaches in Live Cells

A high temporal resolution is required to understand single-molecule dynamics and cell fates in heterogeneous cell populations. To achieve single-mRNA resolution inside living cells, a genetically encoded stem-loop array has been successfully used. The MS2 system exploits a highly specific binding of MS2 capsid protein (MCP) and MS2 binding site (MBS) RNA stem-loop (SL) from MS2 bacteriophage (11). A gene tagged with multiple copies of MS2-SL produces a reporter mRNA that binds MCP-GFP (green fluorescent protein) fusion proteins expressed in the same cell. As a result, each reporter mRNA is labeled with many GFPs and becomes bright enough for single-mRNA imaging in live cells. Tagging an endogenous mRNA with MS2-SL is relatively easy in yeast using homologous recombination (68). Studies in mammalian cells have been done using transient transfection or cells from a β-actin mRNA MBS knock-in mouse (89) and a transgenic mouse expressing MCP-GFP (115). This technique has been extensively used to monitor real-time dynamics of transcription, nuclear export, and trafficking of mRNAs in live cells (reviewed in 20, 114) (Figure 1*a*). Also, recent advances in CRISPR-Cas technology have greatly facilitated genome editing (129) and RNA labeling (108) for live cell imaging.

The evaluation of each aspect of mRNA metabolism has required the development of specific microscopy or analytical tools. For example, one of the great advantages of the MS2-MCP system is that it allows single-molecule tracking of RNA in living cells. The goal of single-particle tracking (SPT) is to assign a specific trajectory to individual mRNAs (Figure 1*b* and Table 1). An important parameter for SPT is the spacing-displacement ratio, which refers to the average distance between particles divided by the average displacement

of a particle between two successive image frames. If this ratio is larger than one, particle tracking can be performed by searching for the nearest neighbor in successive image frames. However, with a lower spacing-displacement ratio, it becomes more difficult to connect the trajectories (114). Thus, various tracking algorithms have been developed to find the most probable set of particle trajectories (31). mRNA molecules exhibit complex dynamics switching between diffusive motion and directional transport (52), which can be analyzed by using a software for inferring transient transport states (75, 101). Simultaneous tracking of single mRNAs and ribosomes by multispectral live cell imaging has revealed that mRNAs loaded with polyribosomes move slower than nontranslating mRNAs (75). This observation was confirmed by simultaneously tracking single mRNA molecules and nascent polypeptides as they are synthesized (155). The translational state of an mRNA is indistinguishable based on its dynamics but can be identified by the visualization of the nascent peptides (103, 150, 155, 157). Another example, discussed below, is the development of a super-registration method that resolves the kinetics of β-actin mRNA export through the nuclear pore complex (NPC) (60). By combining this method with newly developed multifocus microscopy, one can capture 3D single-molecule real-time images and perform an analysis that determines the position as well as the diffusion rate of β-actin mRNAs in the nucleus (134).

The resources to see real-time biological processes, such as transcription and translation, have increased with the design of the orthologous stem-loop systems such as PP7 (27) (Figure 1*a,c*) and other systems like λ boxB RNA (78) or a U1A tag (16, 138) (specific for yeast). Multicolor RNA imaging has been applied to measure transcription elongation by tagging the same mRNA with PP7-SL in the 5′ end and MS2-SL in the 3′ end and quantifying, over time, the fluorescence signal from nascent transcripts binding PP7 coat protein fused to GFP (PCP-GFP) and MCP-mCherry (68). Alternatively, the first round of translation has been localized to single-molecule resolution within a live cell by tagging a single mRNA in the open reading frame (ORF; where the PCP is displaced by translation) and the 3′ untranslated region (3′ UTR), and monitoring where the change from two colors to one color occurs in the cell (63).

Although mRNA is a central molecule to analyzing the regulation of gene expression, gene function is usually performed by proteins. Imaging of single proteins has been limited by the number of photons emitted by one fluorophore. To increase the signal, several solutions have been developed. A repeating peptide array named SunTag has been engineered to recruit multiple copies of an antibody fused to a fluorophore, such as GFP (139) (Figure 1*a*). It is possible to achieve single-molecule resolution for any protein tagged with the SunTag system and track the proteins in live cells (Figure 1*c*). In addition, N-terminal tagging with the SunTag system visualizes the synthesis of a nascent peptide from single mRNAs labeled with the MS2 or PP7 systems (103, 150, 155, 157) (Figure 1*b,c*). An alternative approach has been to use brighter dyes than the conventionally used fluorescent proteins. Especially remarkable for its versatility is the HaloTag technology, a modular tag system based on a modified haloalkane dehalogenase (Halo) from bacteria designed to covalently bind to synthetic ligands (94). This ligand can be a reactive linker attached to a fluorescent dye. The HaloTag fluorescence ligands are at least an order of magnitude brighter than conventional fluorescent proteins like GFP (58). This technology has been extremely useful to perform

SPT of transcription factors (TFs) (discussed below). Additionally, advances in two-photon fluorescence correlation spectroscopy (FCS) have made possible the analysis of single-mRNA and single-protein association in the cell (154). This approach is based on the statistical analysis of fluctuations in fluorescence signals from two molecules of different colors (RNA and protein) when passing through the excited spot. In this application, the total amount of proteins bound to the RNA can be calculated, on the basis of the amount of correlated brightness, by fluorescence fluctuation spectroscopy (FFS) (Figure 1*b*) (154).

Combinations of snapshot and real-time approaches have been used to elucidate different steps of gene expression. To survey the latest advances, we describe recent discoveries on the transcriptional and post-transcriptional processes that regulate gene expression, and the coupling between transcription and mRNA fate.

SINGLE-CELL ANALYSIS OF TRANSCRIPTION

Transcription is the first step of gene expression and a highly regulated process. The state and level of expression of each gene are tightly regulated by complex interactions between DNA sequences, multiple TF concentrations, and target search and chromatin structure remodeling. The stochastic and transient nature of these interactions requires single-cell imaging for a better understanding of the regulation of transcription. Moreover, single-molecule analysis isolates and interrogates the behavior and influence of each of these regulators on the transcriptional output.

Promoter Sequence

A promoter contains specific sequences recognized by TFs to modulate transcription. It is now well established that transcription is inherently stochastic and occurs predominantly as an episodic process or burst (90). Nonetheless, constitutive modes have been described (159) in which transcription is not limited to a short period of time. Characterization of the transcriptional activity by smFISH in yeast has indicated that several transcriptional profiles are encoded by the promoter sequence without being influenced by the genomic locus, gene length, or gene sequence (69). Despite the strong influence of the promoter sequence, transcription from alleles of the same gene is not coordinated in time and strength (68, 89, 141, 147). For example, in mouse embryonic stem cells (ESCs) transcription of *Nanog*, a key regulator of pluripotency, occurs from both alleles in 14% of the cells and 45% of them have only one active allele (141). These observations underscore the stochasticity of transcription and the influence of other regulatory factors.

Transcription Factor Dynamics

TFs transmit information on the cell state and bind to specific DNA sequences on gene promoters to control the rate of transcription by RNA polymerase II (Pol II). Cell-to-cell variation in TF concentration leads to differential cell-fate decisions even within isogenic populations (4, 126, 141). This is especially relevant for ESCs, where heterogeneity provides an advantage to maintain the pluripotency network (141). In addition to concentration, TFs such as ERK, p53, or NF-κB can transfer information through changes in localization rather than global concentration (25, 36, 109, 118). In this case, tracking of fluorescence proteins

in live cells provides a more powerful and robust approach for assessment of TF dynamics than does analysis of fixed cells. For example, p53 fused to a fluorescence protein shows a series of discrete pulses of proteins into the nucleus. The number of pulses varies among cells and the mean of pulses increases with DNA damage, but the individual pulses are of fixed duration and amplitude (77). At the *c-Fos* gene, the TF concentration determines the burst frequency, the duration of TF binding on chromatin affects the burst duration, and the strength of the transactivation domain of TF affects RNA Pol II initiation frequency (126).

Recently, microfluidics coupled to quantitative time-lapse fluorescence microscopy to control TF dynamics and measure the dynamic gene expression response of individual genes have been applied to the analysis of single yeast cells (64, 65, 88, 100). This analysis has revealed that the TF Msn2 determines multiple and distinct gene expression profiles depending on the amplitude threshold and timescale of activation, which is influenced by the nucleosome occupancy (64). Interestingly, the gene expression program interpreted by a specific promoter can be modulated by modifying promoter *cis* elements (65). Moreover, usually several TFs operate simultaneously, and the promoter should integrate different sources of information. In the case of Msn2, it differentially modulates the expression of target genes, depending on the temporal overlap or nonoverlap with the pulse of activity of the transcriptional repressor Mig1 (88). These examples indicate that TF dynamics transmit the information necessary to regulate transcription and therefore require analysis with the proper spatial and temporal resolution.

Transcription Factor Target Search

Ultimately, each TF molecule has to find its specific locus and bind to its target site on genomic DNA to trigger gene expression. Fluorescence recovery after photobleaching (FRAP) and FCS complement each other and provide further detailed information on TF dynamics in the nucleus (23, 117; reviewed in 37, 92). These techniques can extract kinetic parameters on the movement and distribution of proteins and the rate of exchange between different cellular compartments or immobilization of proteins in large structures. They have, for example, established that TF binding to chromatin is generally transient (61) (Figure 1*c*).

Although FCS and FRAP experiments measure the average movement of many molecules, super-resolution fluorescence microscopy allowed the development of SPT techniques for the quantification of TF dynamics with molecular resolution (29, 46, 73, 93). SPT has started to reveal target-search strategies, differentiate specific from nonspecific residence times, and define a hierarchical behavior of TFs in the whole nucleus. In ESCs, Sox2 and Oct4 are essential TFs to maintain pluripotency. Sox2 binds first on the DNA, followed by Oct4. Sox2 locates its cognate binding sites using 3D diffusion (duration ~3 s) followed by 1D sliding along DNA (duration ~0.8 s). Once bound to a cognate recognition site, the average residency time of Sox2 alone is ~12 seconds before it arrests Oct4, which stabilizes the enhanceosome assembly (29). Clusters of Sox2 bound in the nucleus have been localized by a lattice light-sheet–based single-molecule strategy (93). These clusters represent clusters of enhancers and are located in nonheterochromatin regions and overlap with subsets of Pol II.

Interestingly, chromatin structure influences the dynamics of Sox2 (29, 93), and this TF behaves differently in heterochromatic regions and enhancer clusters. Its search mode as well as its distribution change as histone acetylation is globally increased. In particular, histone H3K27 acetylation has been shown to accelerate the search kinetics of TFs and accelerates the transition of Pol II from initiation to elongation (135).

The impact of nuclear architecture on the diffusion of TFs has also been evaluated by tracking two TFs of comparable sizes: c-Myc and positive transcription elongation factor (p-TEFb) (73). These TFs explore the nucleus in different manners. c-Myc moves almost everywhere inside the nucleus (a noncompact exploration), whereas P-TEFb movement is constrained to a specific path through the nucleus (a compact exploration). This geometry-controlled kinetics of exploration could have a strong impact on how TF activity is controlled in space and time in the nucleus (153).

Chromatin Structure and Dynamics

Gene expression requires that gene regulatory elements and coding regions be accessible to TFs and to the transcriptional machinery. The nucleus is a crowded environment with a hierarchy of organized structures in which chromosomes fold into complex 3D conformations (55). Chromosome conformation capture (3C) and 3C-related technologies (4C, 5C, and Hi-C) have allowed the mapping of average intra- and interchromosomal interactions within populations of cells. These technologies, combined with computational modeling, have provided a picture of the topological association of individual domains as well as a genome-wide perspective on functional and structural genomic subdomains in the eukaryotic nucleus (45, 71). These technologies are applied mainly to cell populations and require cross-linking of macromolecular components; thus, they cannot be used to determine the physical distances between interacting regions (8, 107). DNA-FISH is the main alternative for resolving spatial relationships in single cells. Although DNA-FISH can assess only a few loci at the time, it established that chromosomes occupy discrete territories in the cell nucleus (39). In mammalian cells, gene-rich chromosomes generally cluster at the nuclear center, and gene-poor chromosomes frequently localize near the nuclear periphery (152). Moreover, gene-rich regions decorate the outside of their own chromosome territories (15) and certain genes loop outside of their own chromosome territory (152). A recently developed high-throughput 3D mapping platform has unexpectedly shown that DNA replication, rather than mitosis, establishes gene position relative to the nuclear periphery (127). A combination of 5C data, physical modeling, 3D single-molecule DNA, and smFISH for the X chromosome has shown that chromatin structures underlying topological associated domains are highly variable and that these structural fluctuations can contribute to transcription (56).

A limitation of all these methods is that they are applied to fixed cells where dynamic aspects of chromatin organization can only be inferred from snapshots. Tagging of single loci with Lac operon (LacO) arrays with Lac Repressor (LacI) fused to photoactivatable fluorescent protein-tagged histones (102) has demonstrated that chromatin is locally mobile but rarely moves over long distances (105). Nonetheless, the heat shock protein 70 (HSP70) loci move unidirectionally from the nuclear membrane toward nuclear speckles upon

induction of transcription by heat shock in mammalian cells (76). The effect of gene positioning on transcriptional levels is controversial and appears to be organism dependent. Relocation of a specific human chromosome to the nuclear periphery reduces the expression levels of some endogenous human genes located near the tethering sites (51). In contrast, active inducible genes relocate to the NPC in yeast (10, 135). Because most of these studies have been performed using the LacO and LacI system, it is possible that some of the results are biased by such integrations in the genome (43, 74). Recent development of the CRISPR-Cas9 system has produced new tools to follow endogenous sequences. The use of a fluorescently labeled nuclease-deficient Cas9 (dCas9) protein for live imaging of the *MUC4* loci supports the notions that genes assume nonrandom positions and exhibit confined movements at short timescales (28).

Many studies have shown that transcription in the mammalian nucleus occurs at discrete locations. These locations have been called "transcription factories" (137), but the idea of stable transcription factories has been recently challenged. To determine the dynamic nature of these factories, a quantitative single-cell and single-molecule approach has resolved the spatiotemporal organization of Pol II in the nucleus (34). Pol II was fused to the photoswitchable fluorescent protein Dendra2 and examined at single-molecule resolution with PALM. Pol II clusters were found to dynamically assemble and disassemble, with an average lifetime of 5.1 s, supporting a model of self-organizing clustering. Furthermore, these dynamically assembled clusters could explain the long-range chromosomal contacts observed for some co-regulated genes (48). These transient Pol II clusters have been linked to the number of mRNAs synthesized during serum stimulation, suggesting they constitute a pre-transcriptional regulatory event that controls nascent mRNA output (32). The origin of these Pol II clusters remains unknown but could be linked in the future to TF clustering or factors involved in the Pol II preinitiation complex (PIC) assembly.

Transcription Is Predominantly Bursting

It is now well established that transcription predominately occurs in bursts in eukaryotic cells (22, 33, 120, 126, 159), viruses (130), and bacteria (22, 140). Multiple quantitative models have been developed to provide a description of stochastic bursting (79, 120, 126, 159). In the main model, called the telegraphic model, transcription of a gene can switch randomly between an inactive OFF state and an active ON state (Figure 1*c*). While the allele is in the ON state, it can initiate transcription at a specific rate. For example, during serum induction, the TF concentration modulates the burst frequency of *c-Fos* (i.e., the transition between an OFF state and an ON state), but the other parameters, including the rate of initiation by individual Pol II complexes, remain unchanged (126). Steroids also drive the burst frequency of transcription to produce the well-known analog dose response across the population (79). The existence of a transcriptional memory (a period after a burst during which cells cannot switch from the OFF state to the ON state) that lasts up to several hours has been described in mammalian cells (66, 130). Conversely, the social amoeba *Dictyostelium* is more likely to re-express an endogenous developmental gene than initiate new expression (the probability to switch from OFF state to ON state is higher) (33). Large-scale studies suggest that the transcription of a reporter transgene encoding a fluorescent

protein occurs as a burst regardless of its location in the human genome. The frequency and size of the transcriptional burst are equally modulated across the genome (41, 132, 148).

Different steps of transcription can potentially generate bursts. For example, chromatin may switch between a permissive and a repressive state, a TF may bind to a promoter or enhancer, or a loop may be formed so that the PIC can reinitiate transcription (26, 38, 136). Models of transcription regulation have been built after the simultaneous observation of pairs of these regulatory events in fixed and live cells, and the application of correlation techniques to define kinetics and provide models of transcription regulation (38, 56, 76, 80, 111, 126, 135, 156). A better picture of the components orchestrating the spatiotemporal regulation of gene transcription would come with the simultaneous imaging of chromatin, TFs, and mRNA. A step toward observing biological processes in real time has been the visualization of transcript formation by combining the MS2-MCP and PP7-PCP tags in the same transcript (68). The advantage of this technology is that it enables an mRNA to be followed from the genomic site of its transcription to the cytoplasm and can provide valuable understanding of its dynamic response to factors that influence its biogenesis and translation.

COTRANSCRIPTIONAL AND POST-TRANSCRIPTIONAL REGULATION OF GENE EXPRESSION IN THE NUCLEUS

There are multiple *trans* and *cis* elements that regulate the coding capacity and life of an mRNA. A key current challenge is to engineer molecules to emit fluorescent signals that report on each of these steps, from splicing to decay.

mRNA Maturation

Some insights on how and where mRNA splicing occurs have emerged from imaging the process of splicing, achieved by tagging the intronic sequences on the pre-mRNA (Figure 1*c*). Splicing is cotranscriptional, and it takes place, at least partially, at the TS. Kinetic studies have shown that splicing is completed 5 to 10 minutes after transcription, regardless of the length or number of introns (17, 85, 146). The elongation rate of Pol IIhas been described as uncoupled from ongoing splicing, and multiple spliceosome complexes can assemble simultaneously on active TSs (17). The speed of Pol II elongation and the presence of pause sites can result in alternative splicing (24, 44). However, details of splicing differ from gene to gene. For example, dual-color mRNA imaging in living human cells has shown that β-globin mRNA splicing can occur stochastically both before and after transcript release (38).

An mRNA undergoes maturation by processes in addition to splicing. N6-Methyladenosine and the addition of the polyA tail regulate the stability and translation of the mRNA (91, 151). Additionally, mRNA-binding proteins and nuclear assembly factors are cotranscriptionally recruited to form the messenger ribonucleoprotein (mRNP), which needs to be released from the TS after polyadenylation (119). Some mRNA maturation processes take place at the TS and occur during time the transcribed transcripts remain at the TS (approximately 2 minutes) (38), as shown by using probes or inserting the MS2-MCP in the 3′ end of the gene (17, 126). Nonetheless, there are exceptions. For example, to regulate

translation, the CPEB family of proteins modifies the length of the polyA tail of specific mRNAs once in the cytoplasm (151).

Nuclear Diffusion and Export

Translation requires that the mRNPs exit the nucleus. Once released from the TS, it takes the mRNA molecule ~20 minutes to localize in the cytoplasm of mammalian cells (9, 60). The movement of the mRNA in the nucleus has been analyzed by following the trajectories of single mRNAs tagged with the MS2-MCP system. Using a high-speed multifocus microscope for simultaneous imaging of mRNA in 3D and an internal registration marker for the NPC showed that >60% of total β-actin mRNAs localize within 0.5 μm of an NPC. β-actin mRNAs seem to diffuse freely in the nucleus, although the distribution is not uniform (134).

Entry into the cytoplasm requires that the mRNA successfully finds, interacts, and moves through the NPC. A combination of super-registration and high-speed microscopy has resolved the kinetics of mRNA export (60). A three-step model with docking (80 ms), translocation through the NPC (5–20 ms), and release (80 ms) has clarified the steps involved in mRNA export in mammalian cells (60) (Figure 1*c*). These experiments suggested that not all pores are equally active and the transcript scans along pores until it finds one suitable for mRNA export. Interestingly, the pores transporting β-actin are repeatedly active over time (134). These facts suggest that the selection of a specific NPC could be determined by the interaction of proteins of the mRNP and the nuclear basket of the NPC. In yeast, deletion of the gene encoding the nuclear basket protein Mlp1/2 or the mRNA binding protein Nab2 alters the scanning behavior and shortens the residency times inside the NPCs (123). Additionally, cells achieve directionality of export by selectively removing the essential export factor Mex67 from the mRNP, thereby preventing further interaction of the now cytoplasmic mRNP with the NPC (123, 134). Once in the cytoplasm, the mRNPs are confined near the nuclear envelope. This suggests that mRNPs, once exported, remain with multiple NPCs at their cytoplasmic face; most likely, the mRNP composition is remodeled for future events in the cytoplasm (133). Visualization of the interaction between specific RNA-binding proteins (RBPs) and single-mRNA molecules is essential to understanding the metabolism of the mRNA in the cytoplasm.

CYTOPLASMIC DYNAMICS OF mRNA AND REGULATION OF TRANSLATION

Cytoplasmic Mobility and Localization

The composition of mRNPs is dynamic. Some factors associate cotranscriptionally and remain throughout the life of the mRNA and others interact briefly with the mRNA molecule. The stoichiometry of each of these interactions influences the movement, localization, and fate of the mRNA (47). Usually, an mRNA has one or two binding sites for each factor, which makes it especially challenging to localize, follow, and observe these interactions. However, molecular interactions between mRNA and protein have been recently resolved and localized by fluorescence fluctuation spectroscopy (FFC) and heterospecies partition analysis (154) (Table 1) (Figure 1*b,c*). This technology has been used

in cells expressing β-actin mRNA tagged with the MS2-MCP system and the well-characterized binding protein ZBP1, tagged with mCherry. This approach uses a fluorescent spot, generated by a two-photon microscope, to detect the brightness and diffusion of molecules passing through a femtoliter volume (Figure 1*b,c*). Quantitative measurements of the amount of mRNA, amount of ZBP1, and the different locations of their association proved that β-actin mRNA was preferentially bound to ZBP1 at the nuclear periphery, although this interaction did not form at the TS (154). This association supports the well-known function of ZBP1 in mediating localization and translational repression of this mRNA until activation by the proper stimulus (18, 47). The method also correlates association with specific cellular behavior or morphology.

Localization of mRNAs in different cellular compartments is a widespread mechanism to regulate several cellular processes; it is mRNA and cell-type specific. For example, in the yeast *Saccharomyces cerevisiae*, transport of *ASH1* mRNA along the actin cytoskeleton to the bud tip inhibits mating-type switching in the daughter cell (11, 18). In *Drosophila melanogaster* oocytes, *oskar* mRNA is actively transported in ribonucleoprotein granules to be anchored in the posterior end where it is translated (see below) (143). Localization and translational repression in the granules are essential for *Drosophila* development and patterning. Structural illumination microscopy and smFISH have indicated the homotypic distribution of the mRNAs in these granules (143). β-actin mRNA is also packed in neuronal granules to exit the soma and be actively transported in dendrites (19). Synaptic stimulation induces the temporal release of the β-actin–mRNA from the granules, probably to be locally translated and contribute to synaptic plasticity (19, 115). In addition, β-actin mRNA localization in fibroblast protrusions promotes directed cell migration, as shown by an analysis that correlates mRNA localization in a living cell with motility (116). Finally, localization of mRNAs in the cytoplasm also responds to changes in environmental conditions. For example, mRNAs are packed in processing or stress bodies under stress conditions, and after stress the mRNA can be released and return to translation or become degraded (42).

Single-Cell Analysis of Translation: Where, When, and How?

The importance of spatial localization is most apparent in the context of translation. By combining spatial and temporal regulation, the cell allows transcripts to be in the right place at the right time, ensuring that the resulting proteins are used efficiently when needed. This saves cellular resources and prevents possible protein-associated toxicities.

To determine when the pioneer round of translation occurs in mRNAs, the MS2 and PP7 systems have been used to tag the same transcript with two spectrally different fluorescent proteins. The rationale is that the fluorescence signal from the MS2-MCP, inserted in the 3′ UTR, localizes the transcript at all times and the fluorescence signal from the PP7-PCP, inserted in the ORF, is released by the elongating ribosomes melting the PP7-SL. The technique, known as TRICK (translation RNA imaging by coat protein knockoff), is based on the switch from a two- to one-color labeled transcript, therefore distinguishing the moment when mRNA converts from an untranslated to translated state (63) (Figure 1*c*). In mammalian cells, TRICK has confirmed that little translation occurs in the nucleus and that

the pioneer round of translation is completed before the mRNA has diffused more than a few micrometers away. Interestingly, mRNAs sequestered in processing bodies upon stress remain untranslated while trapped (63). Because the method assesses the spatiotemporal control of translation, it has been used to localize the expression of *oskar* in the posterior pole of the *Drosophila* oocyte at stage 10. In this case, the change of the fluorescence labeling of the reporter has been correlated with the detection of the accumulation of the *oskar* protein in the posterior pole (63). To provide further information on translation events, this technique needs to be complemented with live-cell imaging of the translational status of the mRNA after the pioneer round.

To analyze where translation takes place and how it alters the dynamics of mRNAs, one can image both ribosomes and transcripts within the same cell. FFC has been used to determine the association of ribosomes with β-actin transcripts (154). The subsequent heterospecies analysis showed differences in ribosome loading upon individual β-actin transcripts, with a higher number of ribosomes per transcript at the cell periphery. Therefore, association of β-actin transcripts with ZBP1 and ribosomes is anticorrelated, and these results corroborate prior observations that sequestration by ZBP1 leads to translational repression at the nuclear periphery (70). Translation of β-actin at the cell periphery has also been suggested by tracking the comovement of the transcript with labeled ribosomes at high spatiotemporal resolution. HMM-Bayes analysis (Table 1) of the trajectories has indicated the presence of two diffusion states (slow and fast) (75). Transition from slow to fast states correlates with the disappearance of the ribosomal signal (75) (Figure 1*c*). Therefore, this method is a good way to distinguish translating (polysome-associated) from nontranslating transcripts and suggests a burst mode of translation similar to that described for transcription.

This proposition was recently confirmed with a method to directly quantify the number of proteins made per burst of translation and the frequency and speed of translation (103, 150, 155, 157). A major hurdle to accomplishing this has been the observation of single-protein molecules. The diffusion of most proteins is too fast to observe with standard microscopy. Recently, two different approaches have addressed this problem through the use of multiplexed antibody conjugated fluorophores, which not only increase the signal but also decrease the diffusion rate of the target protein. Through the use of Fabs (fragments antigen-binding) targeting either a short peptide epitope or GFP itself, multiple groups have been able to increase the fluorescence intensity from a single protein. Additionally, these techniques detect the nascent peptides as they are being synthesized because they do not require additional maturation time to fluoresce, as is the case for GFP. One example was the development of Spaghetti monster (149), which used exogenous, bead-loaded Fab fragments targeting multimeric HA and FLAG epitopes on a GFP molecule. The use of single-chain variable fragment (scFv) antibodies fused to GFP makes the development of a fully genetically encoded system possible (SunTag). Both systems (Spaghetti monster and SunTag) allowed the addition of 24 × GFPs onto a single target protein, providing a bright enough signal to image translation sites as well as single protein molecules over long periods of time (103, 139, 150, 155, 157) (Figure 1*a,c*). By combining these approaches, mRNAs tagged with the MS2-MCP or PP7-PCP systems have been co-tracked with newly formed proteins within the same translation sites, allowing for a number of observations to be made about translation. The first conclusion is that translation undergoes bursty kinetics (periods

of continuous translation followed by periods of quiescence), much like in transcription (Figure 1*b,c*). After exposure to oxidative stress, global translation decreases; however, some transcripts, such as the stress response transcription factor Atf4, have a sharp and transient increase in translation (150).

Through different combinations of FRAP, drug treatment, and modeling of ribosome runoff after harringtonine treatment, the four studies directly measured ribosome elongation rate (3–10 AA/s) and calculated that ribosomes occur approximately every 200–300 nucleotides on an mRNA (103, 150, 155, 157). Although codon optimization increases the rate of translation, it was also noticed that 5–10% of mRNAs had ribosomes fail to run off because of chemical damage of the mRNA (157). In hippocampal neurons, translation occurs more often in the proximal regions of the neuron and can still happen while the mRNA is moving. Interestingly, visualization of the translational dynamics of ER-targeted mRNAs has shown that tethered mRNAs can be translated only by ER-bound ribosomes, supporting the co-translocon model (155). These studies will pave the way for further insights on translation in different contexts, such as cell cycle regulation, development, and disease.

Single-Cell Analysis of Decay

Finally, at the end of its lifetime, the mRNA molecule has to be degraded. This is a fast and highly regulated process used by cells to quickly adapt their transcriptome to their metabolic requirements. Single-cell analysis has also been used to clarify longstanding debates about the location at which nonsense-mediated decay (NMD) destroys transcripts bearing nonsense codons. SmFISH identified transcripts within the same cell containing either a normal or premature termination codon (PTC) using a bidirectional promoter expressing β-globin (Figure 1*c*). Surprisingly, NMD degradation of the majority of mRNAs that contain a premature stop codon takes place in the cytoplasm and not in the nucleoplasm as suspected (144). Export of these mRNAs is thus not affected by the stop codon. Through the use of TRICK (see above), the pioneer round has been visualized (63); thus, it is now possible to track transcripts that escape NMD, which should give interesting insights into what happens to the small population of surviving transcripts. Results thus far suggest that the small number of transcripts that escape this process appear to have decay rates similar to their normal counterparts (62).

COORDINATION OF TRANSCRIPTION WITH DOWNSTREAM EVENTS OF mRNA LIFE

In contrast to the stochastic activation of transcription, a synchronous switch in the decay rates of cell cycle–regulated mRNAs from $t_{1/2}=90$ min at the G2/M border to $t_{1/2} < 3$ min at anaphase has been documented by smFISH in yeast (142) (Figure 1*c*). Surprisingly, such coordination of decay is independent of the transcript sequence and relies exclusively on the promoter sequence.

Interestingly, single-cell analysis to correlate cell morphology and gene expression has revealed that cytoplasmic mRNA decay rates are promoter dependent but completely independent of transcript sequence (62). These studies modify the view of the regulation of

gene expression to see individual steps as linked by showing that the promoters of cell cycle–regulated genes (*SWI5* and *CBL2*) imprint their transcripts to assure proper degradation timing during cell cycle progression. Similarly, the heat shock element (HSE) in the promoter of stress-regulated genes is the only sequence required to determine whether the transcribed mRNA is translated instead of packaged in stress granules under glucose starvation conditions (160). Continuing the theme of integration of the regulatory steps, the translation elongation factor eEF1A links transcription of the heat shock protein 70 (HSP70) to its translation upon heat shock (147), probably to ensure preferred synthesis of the HSPs.

The robust coordination among transcription, translation, and decay demonstrated for cell cycle– and stress-regulated genes is of obvious utility. We hypothesize that this novel cross talk between the nucleus and the cytoplasm would fine-tune other cellular processes, such as differentiation. In fact, it has been recently reported, although not at the single-cell level, that myoblast differentiation involved the coordination of fibroblast growth factor 1 (FGF1) transcription and translation (1). The splicing factors hnRNPM and p54nrb mediate this process by interacting with promoter elements and binding to the 5′ UTR of the mRNA. Hence, coupling transcription to translation and decay provides an efficient mechanism for the cell to adjust to environmental changes, fulfill its own cell cycle, and specialize by differentiation.

PERSPECTIVES GAINED FROM SINGLE-CELL ANALYSIS

Single-cell analysis has changed our understanding of how gene expression is regulated and provided new technologies for studying this process. Numerous fields in biology have taken advantage of these technologies to characterize rare populations of cells or study the cell-to-cell variability of gene expression within individual populations of cells and multicellular organisms. Here, we discuss these advantages with recent examples.

Cell-to-Cell Heterogeneity: Noise in Gene Expression

Single-cell analysis of gene expression has revealed significant variations among cells. This variation, defined as noise, refers to heterogeneity in a population of isogenic cells that cannot be explained by the low rate of mutation. Noise can be of extrinsic or intrinsic origin (106). Extrinsic noise derives from environmental fluctuations, arbitrary partitioning of molecules between daughter cells, or cell size. It is relatively easy to picture that cells in a population could be differentially exposed to environmental changes and therefore respond differently to a stimulus. Intrinsic noise, derived from the stochasticity of transcription and translation, could enhance or compensate the diversification of the response (40, 98). For example, increases in cell volume are accompanied by adjustments in transcriptional burst size and frequency during the cell cycle (113). At essential genes that encode products needed to operate at defined concentrations, highly bursty transcription is compensated by inefficient mRNA translation to achieve low intrinsic noise (83).

Nuclear retention of specific mRNAs represents an alternative mode of regulation that allows cells to express proper protein levels independent of transcription and translation (2). Although transcription in metazoan cells is mainly stochastic, the cytoplasmic content of mRNAs can be determined, considering both the cellular phenotypic state and context (7).

These experiments uncovered a new function for the nuclear envelope: to buffer the transcriptional noise in the cytoplasm of higher eukaryote cells. It still remains to be determined whether this or other mechanisms represent an evolutionary path to control noise in gene expression programs required for proper functioning in multicellular organisms.

Single-Cell Analysis in Multicellular Organisms: Spatiotemporal Resolution of Cell-to-Cell Variability

In multicellular organisms, each cell must adapt its transcriptome and proteome to the demands of the whole organism. One example of such adaptation is the liver, which absorbs glucose after a meal and synthesizes and releases glucose during starvation (3). SmFISH has revealed that hepatocytes switch from glucose absorbers to secreters by coordinating transcription and mRNA decay of the gluconeogenic genes *Pck1* and *G6pc*. During fasting states, gluconeogenic genes achieve higher levels of expression by a synchronized increase of the transcriptional burst and decrease of mRNA degradation rates. This synchronization also allows for a prompt degradation of transcripts to adapt to the fast increase in glucose levels after meals. Surprisingly, there is a high heterogeneity in the transcriptional output among hepatocytes. This cell-to-cell variability also applies to other genes considered constitutive, such as *β-actin*. In the case of *β-actin*, transcription is burstier and the mRNAs are more stable. Interestingly, polyploid hepatocytes are less noisy than diploid ones. Hence, a combination of cell polyploidy and regulation of the mRNA half-life seems to control transcriptional noise in the liver (3).

The heterogeneous transcription among cells must be shaped to ensure tissue functionality and development. In the case of the pituitary gland, the length and intensity of the prolactin transcriptional burst become shorter and less intense over age and the frequency is slightly unchanged. Interestingly, in the adult gland, cells that are proximal to each other have a better coordination in expression than distal ones, suggesting a role of the spatial organization and inter-cellular communication in dampening the noise (49).

The most noteworthy example of gene expression coordination occurs during embryogenesis. From fertilization, gene expression is tightly delimited in time and space to determine the identity and fate of each individual cell and to orchestrate the formation of the new body. The MS2 system provides the ability to image individual cells in the whole *Drosophila* embryo, unraveling spatiotemporal and mechanistic insights behind its development (57). Three hours after fertilization, the *Drosophila* embryo is composed of ~6,000 cells with pattern formation information that determines the *Drosophila* body segments (81). The maternal mRNA *bicoid* (*bcd*) determines the anterior-posterior axis by activating the gene *hunchback* (*hb*) in a protein gradient–dependent manner. The formation of this sharp boundary between *hb*-expressing and -nonexpressing cells has been characterized in real time by monitoring the activity of the *hb* promoter with the MS2-MCP system (53, 97). Interestingly, cells in the posterior initiate transcription at the same time as cells in the anterior, but the concentration of the BCD protein determines the strength and length of transcription. Spontaneous activation of the *hb* promoter becomes repressed in the posterior from nuclear division 11. It is also remarkable that all active cells exhibit synchronized initiation of transcription after mitosis and that once transcription is on in a

cell, there is a single peak of activity (53, 97). This deterministic expression differs from the highly variable bursty profile displayed by the even-skipped (*eve*) stripe 2 gene. Remarkably, this well-defined pattern shows a broad activation in interphase of nuclear divisions 11 to 13, which is refined to the stripes at cellularization and disappears at gastrulation (13).

These examples highlight the relevance of visualizing individual cells and their activity over time to unmask mechanisms such as *Drosophila* pattering. Nonetheless, this strategy has only begun to characterize the initial processes in the life of a multicellular organism. In *Drosophila*, the complex interaction of ~1,000 enhancers defines the activity of a few genes. The strategies used to examine single enhancers and promoters at the *hb* and *eve* stripe 2 genes, cited above, have been extended to characterize the interplay of pairs of enhancers for *hb*, *kni*, and *sna* promoters. Each case showed its own individual scenario to reach precise and reliable levels of expression (14).

If there are many combinations of factors to consider, it is necessary to integrate thousands of experiments to take into account the variability of gene expression. Hence, it is a necessity to explore new technologies that will allow the visualization of hundreds of genes at once. These experiments must consider not only transcription, the first step of gene expression, but also post-transcriptional regulatory events that control localization, stability, and translation of an mRNA.

Single-Cell Analysis in Rare Cells: Role of Stem Cells in Tissue Homeostasis

Single-cell analysis has the unique advantage of being able to characterize low-abundance cells, such as stem cells, in the context of their environment (145). A representative example is the LGR5$^+$ epithelial stem cells that orchestrate the homeostasis of the small intestine. Tracking of differentially labeled stem cells has resolved the structure, dynamics, and plasticity of the small intestine in time and space, and provided a platform to analyze the expression patterns of individual cells (35). This has been done by two complementary methods: smFISH in tissue and RNA-seq. SmFISH has revealed the spatial distribution of stem cell markers in the crypt, regulatory coexpression of transcripts, and changes in expression upon irradiation. Interestingly, cell positioning in the tissue defines its pattern of gene expression, which is similar among intestinal crypts and mice and over time (59, 72). The most relevant consequence of these single-cell studies is their therapeutic implications. In vitro production of mini-guts from single stem cells facilitates the regeneration of the damaged intestine and sheds light on the molecular origin of adenocarcinoma (124).

CONCLUSIONS AND REMARKS

The development of novel single-cell and single-molecule imaging technologies and analysis tools has repositioned biological questions on gene expression regulation. Every cell undergoes constant changes to fulfill the requirements of its cell cycle, to differentiate, and to respond to external stimulus. The precise execution of these cell programs requires the flexibility provided by dynamic interactions among many molecules. Quantification of the contribution of each component to a specific biological function has been made possible by the spatiotemporal resolution offered by fluorescence microscopy and the analysis of individual cells. Technologies have been adapted to test biological questions from the

models that have been created to explain particular pathways. Synergistic efforts from different disciplines from biology to engineering will continue to provide new tools to understand the cell's metabolism and the evolution of multicellular organisms.

Acknowledgments

References

1. Ainaoui N, Hantelys F, Renaud-Gabardos E, Bunel M, Lopez F, et al. Promoter-dependent translation controlled by p54nrb and hnRNPM during myoblast differentiation. PLOS ONE. 2015; 10:e0136466. [PubMed: 26332123]

2. Bahar Halpern K, Caspi I, Lemze D, Levy M, Landen S, et al. Nuclear retention of mRNA in mammalian tissues. Cell Rep. 2015; 13:2653–62. [PubMed: 26711333]

3. Bahar Halpern K, Tanami S, Landen S, Chapal M, Szlak L, et al. Bursty gene expression in the intact mammalian liver. Mol Cell. 2015; 58:147–56. [PubMed: 25728770]

4. Balazsi G, van Oudenaarden A, Collins JJ. Cellular decision making and biological noise: from microbes to mammals. Cell. 2011; 144:910–25. [PubMed: 21414483]

5. Bandura DR, Baranov VI, Ornatsky OI, Antonov A, Kinach R, et al. Mass cytometry: technique for real time single cell multitarget immunoassay based on inductively coupled plasma time-of-flight mass spectrometry. Anal Chem. 2009; 81:6813–22. [PubMed: 19601617]

6. Battich N, Stoeger T, Pelkmans L. Image-based transcriptomics in thousands of single human cells at single-molecule resolution. Nat Methods. 2013; 10:1127–33. [PubMed: 24097269]

7. Battich N, Stoeger T, Pelkmans L. Control of transcript variability in single mammalian cells. Cell. 2015; 163:1596–610. [PubMed: 26687353]

8. Belmont AS. Large-scale chromatin organization: the good, the surprising, and the still perplexing. Curr Opin Cell Biol. 2014; 26:69–78. [PubMed: 24529248]

9. Ben-Ari Y, Brody Y, Kinor N, Mor A, Tsukamoto T, et al. The life of an mRNA in space and time. J Cell Sci. 2010; 123:1761–74. [PubMed: 20427315]

10. Berger AB, Cabal GG, Fabre E, Duong T, Buc H, et al. High-resolution statistical mapping reveals gene territories in live yeast. Nat Methods. 2008; 5:1031–37. [PubMed: 18978785]

11. Bertrand E, Chartrand P, Schaefer M, Shenoy SM, Singer RH, Long RM. Localization of ASH1 mRNA particles in living yeast. Mol Cell. 1998; 2:437–45. [PubMed: 9809065]

12. Betzig E, Patterson GH, Sougrat R, Lindwasser OW, Olenych S, et al. Imaging intracellular fluorescent proteins at nanometer resolution. Science. 2006; 313:1642–45. [PubMed: 16902090]

13. Bothma JP, Garcia HG, Esposito E, Schlissel G, Gregor T, Levine M. Dynamic regulation of eve stripe 2 expression reveals transcriptional bursts in living *Drosophila* embryos. PNAS. 2014; 111:10598–603. [PubMed: 24994903]

14. Bothma JP, Garcia HG, Ng S, Perry MW, Gregor T, Levine M. Enhancer additivity and non-additivity are determined by enhancer strength in the *Drosophila* embryo. eLife. 2015; 4:e07956.

15. Boyle S, Rodesch MJ, Halvensleben HA, Jeddeloh JA, Bickmore WA. Fluorescence in situ hybridization with high-complexity repeat-free oligonucleotide probes generated by massively parallel synthesis. Chromosome Res. 2011; 19:901–9. [PubMed: 22006037]

16. Brodsky AS, Silver PA. Identifying proteins that affect mRNA localization in living cells. Methods. 2002; 26:151–55. [PubMed: 12054891]

17. Brody Y, Shav-Tal Y. Transcription and splicing: when the twain meet. Transcription. 2011; 2:216–20. [PubMed: 22231117]

18. Buxbaum AR, Haimovich G, Singer RH. In the right place at the right time: visualizing and understanding mRNA localization. Nat Rev Mol Cell Biol. 2015; 16:95–109. [PubMed: 25549890]

19. Buxbaum AR, Wu B, Singer RH. Single β-actin mRNA detection in neurons reveals a mechanism for regulating its translatability. Science. 2014; 343:419–22. [PubMed: 24458642]

20. Buxbaum AR, Yoon YJ, Singer RH, Park HY. Single-molecule insights into mRNA dynamics in neurons. Trends Cell Biol. 2015; 25:468–75. [PubMed: 26052005]

21. Cabili MN, Dunagin MC, McClanahan PD, Biaesch A, Padovan-Merhar O, et al. Localization and abundance analysis of human lncRNAs at single-cell and single-molecule resolution. Genome Biol. 2015; 16:20. [PubMed: 25630241]

22. Cai L, Dalal CK, Elowitz MB. Frequency-modulated nuclear localization bursts coordinate gene regulation. Nature. 2008; 455:485–90. [PubMed: 18818649]

23. Capoulade J, Wachsmuth M, Hufnagel L, Knop M. Quantitative fluorescence imaging of protein diffusion and interaction in living cells. Nat Biotechnol. 2011; 29:835–39. [PubMed: 21822256]

24. Carrillo Oesterreich F, Bieberstein N, Neugebauer KM. Pause locally, splice globally. Trends Cell Biol. 2011; 21:328–35. [PubMed: 21530266]

25. Caunt CJ, McArdle CA. ERK phosphorylation and nuclear accumulation: insights from single-cell imaging. Biochem Soc Trans. 2012; 40:224–29. [PubMed: 22260695]

26. Chalancon G, Ravarani CN, Balaji S, Martinez-Arias A, Aravind L, et al. Interplay between gene expression noise and regulatory network architecture. Trends Genet. 2012; 28:221–32. [PubMed: 22365642]

27. Chao JA, Patskovsky Y, Almo SC, Singer RH. Structural basis for the coevolution of a viral RNA-protein complex. Nat Struct Mol Biol. 2008; 15:103–5. [PubMed: 18066080]

28. Chen B, Gilbert LA, Cimini BA, Schnitzbauer J, Zhang W, et al. Dynamic imaging of genomic loci in living human cells by an optimized CRISPR/Cas system. Cell. 2013; 155:1479–91. [PubMed: 24360272]

29. Chen J, Zhang Z, Li L, Chen BC, Revyakin A, et al. Single-molecule dynamics of enhanceosome assembly in embryonic stem cells. Cell. 2014; 156:1274–85. [PubMed: 24630727]

30. Chen KH, Boettiger AN, Moffitt JR, Wang S, Zhuang X. RNA imaging. Spatially resolved, highly multiplexed RNA profiling in single cells. Science. 2015; 348:aaa6090. [PubMed: 25858977]

31. Chenouard N, Smal I, de Chaumont F, Maska M, Sbalzarini IF, et al. Objective comparison of particle tracking methods. Nat Methods. 2014; 11:281–89. [PubMed: 24441936]

32. Cho WK, Jayanth N, English BP, Inoue T, Andrews JO, et al. RNA polymerase II cluster dynamics predict mRNA output in living cells. eLife. 2016; 5:e13617. [PubMed: 27138339]

33. Chubb JR, Trcek T, Shenoy SM, Singer RH. Transcriptional pulsing of a developmental gene. Curr Biol. 2006; 16:1018–25. [PubMed: 16713960]

34. Cisse II, Izeddin I, Causse SZ, Boudarene L, Senecal A, et al. Real-time dynamics of RNA polymerase II clustering in live human cells. Science. 2013; 341:664–67. [PubMed: 23828889]

35. Clevers H. The intestinal crypt, a prototype stem cell compartment. Cell. 2013; 154:274–84. [PubMed: 23870119]

36. Cohen-Saidon C, Cohen AA, Sigal A, Liron Y, Alon U. Dynamics and variability of ERK2 response to EGF in individual living cells. Mol Cell. 2009; 36:885–93. [PubMed: 20005850]

37. Coleman RA, Liu Z, Darzacq X, Tjian R, Singer RH, Lionnet T. Imaging transcription: past, present, and future. Cold Spring Harb Symp Quant Biol. 2016; doi: 10.1101/sqb.2015.80.02720

38. Coulon A, Ferguson ML, de Turris V, Palangat M, Chow CC, Larson DR. Kinetic competition during the transcription cycle results in stochastic RNA processing. eLife. 2014; 3:e03939.

39. Cremer T, Cremer C. Chromosome territories, nuclear architecture and gene regulation in mammalian cells. Nat Rev Genet. 2001; 2:292–301. [PubMed: 11283701]

40. Dacheux E, Firczuk H, McCarthy JE. Rate control in yeast protein synthesis at the population and single-cell levels. Biochem Soc Trans. 2015; 43:1266–70. [PubMed: 26614671]

41. Dar RD, Razooky BS, Singh A, Trimeloni TV, McCollum JM, et al. Transcriptional burst frequency and burst size are equally modulated across the human genome. PNAS. 2012; 109:17454–59. [PubMed: 23064634]

42. Decker CJ, Parker R. P-bodies and stress granules: possible roles in the control of translation and mRNA degradation. Cold Spring Harb Perspect Biol. 2012; 4:a012286. [PubMed: 22763747]

43. Dubarry M, Loiodice I, Chen CL, Thermes C, Taddei A. Tight protein-DNA interactions favor gene silencing. Genes Dev. 2011; 25:1365–70. [PubMed: 21724830]

44. Dujardin G, Lafaille C, de la Mata M, Marasco LE, Munoz MJ, et al. How slow RNA polymerase II elongation favors alternative exon skipping. Mol Cell. 2014; 54:683–90. [PubMed: 24793692]

45. Ea V, Baudement MO, Lesne A, Forne T. Contribution of topological domains and loop formation to 3D chromatin organization. Genes (Basel). 2015; 6:734–50. [PubMed: 26226004]

46. Elf J, Li GW, Xie XS. Probing transcription factor dynamics at the single-molecule level in a living cell. Science. 2007; 316:1191–94. [PubMed: 17525339]

47. Eliscovich C, Buxbaum AR, Katz ZB, Singer RH. mRNA on the move: the road to its biological destiny. J Biol Chem. 2013; 288:20361–68. [PubMed: 23720759]

48. Fanucchi S, Shibayama Y, Burd S, Weinberg MS, Mhlanga MM. Chromosomal contact permits transcription between coregulated genes. Cell. 2013; 155:606–20. [PubMed: 24243018]

49. Featherstone K, Hey K, Momiji H, McNamara AV, Patist AL, et al. Spatially coordinated dynamic gene transcription in living pituitary tissue. eLife. 2016; 5:e0894.

50. Femino AM, Fay FS, Fogarty K, Singer RH. Visualization of single RNA transcripts in situ. Science. 1998; 280:585–90. [PubMed: 9554849]

51. Finlan LE, Sproul D, Thomson I, Boyle S, Kerr E, et al. Recruitment to the nuclear periphery can alter expression of genes in human cells. PLOS Genet. 2008; 4:e1000039. [PubMed: 18369458]

52. Fusco D, Accornero N, Lavoie B, Shenoy SM, Blanchard JM, et al. Single mRNA molecules demonstrate probabilistic movement in living mammalian cells. Curr Biol. 2003; 13:161–67. [PubMed: 12546792]

53. Garcia HG, Tikhonov M, Lin A, Gregor T. Quantitative imaging of transcription in living *Drosophila* embryos links polymerase activity to patterning. Curr Biol. 2013; 23:2140–45. [PubMed: 24139738]

54. Gebhardt JC, Suter DM, Roy R, Zhao ZW, Chapman AR, et al. Single-molecule imaging of transcription factor binding to DNA in live mammalian cells. Nat Methods. 2013; 10:421–26. [PubMed: 23524394]

55. Gibcus JH, Dekker J. The hierarchy of the 3D genome. Mol Cell. 2013; 49:773–82. [PubMed: 23473598]

56. Giorgetti L, Galupa R, Nora EP, Piolot T, Lam F, et al. Predictive polymer modeling reveals coupled fluctuations in chromosome conformation and transcription. Cell. 2014; 157:950–63. [PubMed: 24813616]

57. Gregor T, Garcia HG, Little SC. The embryo as a laboratory: quantifying transcription in. Drosophila Trends Genet. 2014; 30:364–75. [PubMed: 25005921]

58. Grimm JB, English BP, Chen J, Slaughter JP, Zhang Z, et al. A general method to improve fluorophores for live-cell and single-molecule microscopy. Nat Methods. 2015; 12:244–50. [PubMed: 25599551]

59. Grun D, Lyubimova A, Kester L, Wiebrands K, Basak O, et al. Single-cell messenger RNA sequencing reveals rare intestinal cell types. Nature. 2015; 525:251–55. [PubMed: 26287467]

60. Grunwald D, Singer RH. In vivo imaging of labelled endogenous β-actin mRNA during nucleocytoplasmic transport. Nature. 2010; 467:604–7. [PubMed: 20844488]

61. Hager GL, McNally JG, Misteli T. Transcription dynamics. Mol Cell. 2009; 35:741–53. [PubMed: 19782025]

62. Haimovich G, Choder M, Singer RH, Trcek T. The fate of the messenger is pre-determined: a new model for regulation of gene expression. Biochim Biophys Acta. 2013; 1829:643–53. [PubMed: 23337853]

63. Halstead JM, Lionnet T, Wilbertz JH, Wippich F, Ephrussi A, et al. Translation. An RNA biosensor for imaging the first round of translation from single cells to living animals. Science. 2015; 347:1367–671. [PubMed: 25792328]

64. Hansen AS, O'Shea EK. Promoter decoding of transcription factor dynamics involves a trade-off between noise and control of gene expression. Mol Syst Biol. 2013; 9:704. [PubMed: 24189399]

65. Hansen AS, O'Shea EK. Limits on information transduction through amplitude and frequency regulation of transcription factor activity. eLife. 2015; 4:e06559.

66. Harper CV, Finkenstadt B, Woodcock DJ, Friedrichsen S, Semprini S, et al. Dynamic analysis of stochastic transcription cycles. PLOS Biol. 2011; 9:e1000607. [PubMed: 21532732]

67. Hess ST, Girirajan TP, Mason MD. Ultra-high resolution imaging by fluorescence photoactivation localization microscopy. Biophys J. 2006; 91:4258–72. [PubMed: 16980368]

68. Hocine S, Raymond P, Zenklusen D, Chao JA, Singer RH. Single-molecule analysis of gene expression using two-color RNA labeling in live yeast. Nat Methods. 2013; 10:119–21. [PubMed: 23263691]

69. Hocine S, Vera M, Zenklusen D, Singer RH. Promoter-autonomous functioning in a controlled environment using single molecule FISH. Sci Rep. 2015; 5:9934. [PubMed: 26017315]

70. Huttelmaier S, Zenklusen D, Lederer M, Dictenberg J, Lorenz M, et al. Spatial regulation of β-actin translation by Src-dependent phosphorylation of ZBP1. Nature. 2005; 438:512–15. [PubMed: 16306994]

71. Imakaev MV, Fudenberg G, Mirny LA. Modeling chromosomes: beyond pretty pictures. FEBS Lett. 2015; 589:3031–36. [PubMed: 26364723]

72. Itzkovitz S, Lyubimova A, Blat IC, Maynard M, van Es J, et al. Single-molecule transcript counting of stem-cell markers in the mouse intestine. Nat Cell Biol. 2012; 14:106–14.

73. Izeddin I, Recamier V, Bosanac L, Cisse II, Boudarene L, et al. Single-molecule tracking in live cells reveals distinct target-search strategies of transcription factors in the nucleus. eLife. 2014; 3:e02230.

74. Jegou T, Chung I, Heuvelman G, Wachsmuth M, Gorisch SM, et al. Dynamics of telomeres and promyelocytic leukemia nuclear bodies in a telomerase-negative human cell line. Mol Biol Cell. 2009; 20:2070–82. [PubMed: 19211845]

75. Katz ZB, English BP, Lionnet T, Yoon YJ, Monnier N, et al. Mapping translation "hot-spots" in live cells by tracking single molecules of mRNA and ribosomes. eLife. 2016; 5:310415.

76. Khanna N, Hu Y, Belmont AS. HSP70 transgene directed motion to nuclear speckles facilitates heat shock activation. Curr Biol. 2014; 24:1138–44. [PubMed: 24794297]

77. Lahav G, Rosenfeld N, Sigal A, Geva-Zatorsky N, Levine AJ, et al. Dynamics of the p53-Mdm2 feedback loop in individual cells. Nat Genet. 2004; 36:147–50. [PubMed: 14730303]

78. Lange S, Katayama Y, Schmid M, Burkacky O, Brauchle C, et al. Simultaneous transport of different localized mRNA species revealed by live-cell imaging. Traffic. 2008; 9:1256–67. [PubMed: 18485054]

79. Larson DR, Fritzsch C, Sun L, Meng X, Lawrence DS, Singer RH. Direct observation of frequency modulated transcription in single cells using light activation. eLife. 2013; 2:e00750. [PubMed: 24069527]

80. Larson DR, Singer RH, Zenklusen D. A single molecule view of gene expression. Trends Cell Biol. 2009; 19:630–37. [PubMed: 19819144]

81. Lecuyer E, Yoshida H, Parthasarathy N, Alm C, Babak T, et al. Global analysis of mRNA localization reveals a prominent role in organizing cellular architecture and function. Cell. 2007; 131:174–87. [PubMed: 17923096]

82. Lee JH, Daugharthy ER, Scheiman J, Kalhor R, Yang JL, et al. Highly multiplexed subcellular RNA sequencing in situ. Science. 2014; 343:1360–63. [PubMed: 24578530]

83. Lehner B. Selection to minimise noise in living systems and its implications for the evolution of gene expression. Mol Syst Biol. 2008; 4:170. [PubMed: 18319722]

84. Levesque MJ, Ginart P, Wei Y, Raj A. Visualizing SNVs to quantify allele-specific expression in single cells. Nat Methods. 2013; 10:865–67. [PubMed: 23913259]

85. Levesque MJ, Raj A. Single-chromosome transcriptional profiling reveals chromosomal gene expression regulation. Nat Methods. 2013; 10:246–48. [PubMed: 23416756]

86. Levsky JM, Shenoy SM, Pezo RC, Singer RH. Single-cell gene expression profiling. Science. 2002; 297:836–40. [PubMed: 12161654]

87. Lidstrom ME, Konopka MC. The role of physiological heterogeneity in microbial population behavior. Nat Chem Biol. 2010; 6:705–12. [PubMed: 20852608]

88. Lin Y, Sohn CH, Dalal CK, Cai L, Elowitz MB. Combinatorial gene regulation by modulation of relative pulse timing. Nature. 2015; 527:54–58. [PubMed: 26466562]

89. Lionnet T, Czaplinski K, Darzacq X, Shav-Tal Y, Wells AL, et al. A transgenic mouse for in vivo detection of endogenous labeled mRNA. Nat Methods. 2011; 8:165–70. [PubMed: 21240280]

90. Lionnet T, Singer RH. Transcription goes digital. EMBO Rep. 2012; 13:313–21. [PubMed: 22410830]

91. Liu N, Pan T. N-methyladenosine-encoded epitranscriptomics. Nat Struct Mol Biol. 2016; 23:98–102. [PubMed: 26840897]

92. Liu Z, Lavis LD, Betzig E. Imaging live-cell dynamics and structure at the single-molecule level. Mol Cell. 2015; 58:644–59. [PubMed: 26000849]

93. Liu Z, Legant WR, Chen BC, Li L, Grimm JB, et al. 3D imaging of Sox2 enhancer clusters in embryonic stem cells. eLife. 2014; 3:e04236. [PubMed: 25537195]

94. Los GV, Encell LP, McDougall MG, Hartzell DD, Karassina N, et al. HaloTag: a novel protein labeling technology for cell imaging and protein analysis. ACS Chem Biol. 2008; 3:373–82. [PubMed: 18533659]

95. Lubeck E, Cai L. Single-cell systems biology by super-resolution imaging and combinatorial labeling. Nat Methods. 2012; 9:743–48. [PubMed: 22660740]

96. Lubeck E, Coskun AF, Zhiyentayev T, Ahmad M, Cai L. Single-cell in situ RNA profiling by sequential hybridization. Nat Methods. 2014; 11:360–61. [PubMed: 24681720]

97. Lucas T, Ferraro T, Roelens B, De Las Heras Chanes J, Walczak AM, et al. Live imaging of bicoid-dependent transcription in *Drosophila* embryos. Curr Biol. 2013; 23:2135–39. [PubMed: 24139736]

98. Maheshri N, O'Shea EK. Living with noisy genes: how cells function reliably with inherent variability in gene expression. Annu Rev Biophys Biomol Struct. 2007; 36:413–34. [PubMed: 17477840]

99. Mazza D, Abernathy A, Golob N, Morisaki T, McNally JG. A benchmark for chromatin binding measurements in live cells. Nucleic Acids Res. 2012; 40:e119. [PubMed: 22844090]

100. Miermont A, Waharte F, Hu S, McClean MN, Bottani S, et al. Severe osmotic compression triggers a slowdown of intracellular signaling, which can be explained by molecular crowding. PNAS. 2013; 110:5725–30. [PubMed: 23493557]

101. Monnier N, Barry Z, Park HY, Su KC, Katz Z, et al. Inferring transient particle transport dynamics in live cells. Nat Methods. 2015; 12:838–40. [PubMed: 26192083]

102. Mora-Bermudez F, Ellenberg J. Measuring structural dynamics of chromosomes in living cells by fluorescence microscopy. Methods. 2007; 41:158–67. [PubMed: 17189858]

103. Morisaki T, Lyon K, DeLuca KF, DeLuca JG, English BP, et al. Real-time quantification of single RNA translation dynamics in living cells. Science. 2016; 352:1425–29. [PubMed: 27313040]

104. Mueller F, Senecal A, Tantale K, Marie-Nelly H, Ly N, et al. FISH-quant: automatic counting of transcripts in 3D FISH images. Nat Methods. 2013; 10:277–78. [PubMed: 23538861]

105. Muller I, Boyle S, Singer RH, Bickmore WA, Chubb JR. Stable morphology, but dynamic internal reorganisation, of interphase human chromosomes in living cells. PLOS ONE. 2010; 5:e11560. [PubMed: 20644634]

106. Munsky B, Neuert G, van Oudenaarden A. Using gene expression noise to understand gene regulation. Science. 2012; 336:183–87. [PubMed: 22499939]

107. Nagano T, Lubling Y, Stevens TJ, Schoenfelder S, Yaffe E, et al. Single-cell Hi-C reveals cell-to-cell variability in chromosome structure. Nature. 2013; 502:59–64. [PubMed: 24067610]

108. Nelles DA, Fang MY, O'Connell MR, Xu JL, Markmiller SJ, et al. Programmable RNA tracking in live cells with CRISPR/Cas9. Cell. 2016; 165:488–496. [PubMed: 26997482]

109. Nelson DE, Ihekwaba AE, Elliott M, Johnson JR, Gibney CA, et al. Oscillations in NF-κB signaling control the dynamics of gene expression. Science. 2004; 306:704–8. [PubMed: 15499023]

110. Novick A, Weiner M. Enzyme induction as an all-or-none phenomenon. PNAS. 1957; 43:553–66. [PubMed: 16590055]

111. Ochiai H, Sugawara T, Yamamoto T. Simultaneous live imaging of the transcription and nuclear position of specific genes. Nucleic Acids Res. 2015; 43:e127. [PubMed: 26092696]

112. Oddone A, Vilanova IV, Tam J, Lakadamyali M. Super-resolution imaging with stochastic single-molecule localization: concepts, technical developments, and biological applications. Microsc Res Tech. 2014; 77:502–9. [PubMed: 24616244]

113. Padovan-Merhar O, Nair GP, Biaesch AG, Mayer A, Scarfone S, et al. Single mammalian cells compensate for differences in cellular volume and DNA copy number through independent global transcriptional mechanisms. Mol Cell. 2015; 58:339–52. [PubMed: 25866248]

114. Park HY, Buxbaum AR, Singer RH. Single mRNA tracking in live cells. Methods Enzymol. 2010; 472:387–406. [PubMed: 20580973]

115. Park HY, Lim H, Yoon YJ, Follenzi A, Nwokafor C, et al. Visualization of dynamics of single endogenous mRNA labeled in live mouse. Science. 2014; 343:422–24. [PubMed: 24458643]

116. Park HY, Trcek T, Wells AL, Chao JA, Singer RH. An unbiased analysis method to quantify mRNA localization reveals its correlation with cell motility. Cell Rep. 2012; 1:179–84. [PubMed: 22832165]

117. Phair RD, Misteli T. High mobility of proteins in the mammalian cell nucleus. Nature. 2000; 404:604–9. [PubMed: 10766243]

118. Purvis JE, Lahav G. Encoding and decoding cellular information through signaling dynamics. Cell. 2013; 152:945–56. [PubMed: 23452846]

119. Qu X, Lykke-Andersen S, Nasser T, Saguez C, Bertrand E, et al. Assembly of an export-competent mRNP is needed for efficient release of the 3′-end processing complex after polyadenylation. Mol Cell Biol. 2009; 29:5327–38. [PubMed: 19635808]

120. Raj A, Peskin CS. The influence of chromosome flexibility on chromosome transport during anaphase A. PNAS. 2006; 103:5349–54. [PubMed: 16567616]

121. Raj A, van den Bogaard P, Rifkin SA, van Oudenaarden A, Tyagi S. Imaging individual mRNA molecules using multiple singly labeled probes. Nat Methods. 2008; 5:877–79. [PubMed: 18806792]

122. Rust MJ, Bates M, Zhuang X. Sub-diffraction-limit imaging by stochastic optical reconstruction microscopy (STORM). Nat Methods. 2006; 3:793–95. [PubMed: 16896339]

123. Saroufim MA, Bensidoun P, Raymond P, Rahman S, Krause MR, et al. The nuclear basket mediates perinuclear mRNA scanning in budding yeast. J Cell Biol. 2015; 211:1131–40. [PubMed: 26694838]

124. Sato T, Clevers H. Growing self-organizing mini-guts from a single intestinal stem cell: mechanism and applications. Science. 2013; 340:1190–94. [PubMed: 23744940]

125. Semrau S, Crosetto N, Bienko M, Boni M, Bernasconi P, et al. FuseFISH: robust detection of transcribed gene fusions in single cells. Cell Rep. 2014; 6:18–23. [PubMed: 24373969]

126. Senecal A, Munsky B, Proux F, Ly N, Braye FE, et al. Transcription factors modulate c-Fos transcriptional bursts. Cell Rep. 2014; 8:75–83. [PubMed: 24981864]

127. Shachar S, Voss TC, Pegoraro G, Sciascia N, Misteli T. Identification of gene positioning factors using high-throughput imaging mapping. Cell. 2015; 162:911–23. [PubMed: 26276637]

128. Shaffer SM, Wu MT, Levesque MJ, Raj A. Turbo FISH: a method for rapid single molecule RNA FISH. PLOS ONE. 2013; 8:e75120. [PubMed: 24066168]

129. Shalem O, Sanjana NE, Zhang F. High-throughput functional genomics using CRISPR-Cas9. Nat Rev Genet. 2015; 16:299–311. [PubMed: 25854182]

130. Singh A, Razooky B, Cox CD, Simpson ML, Weinberger LS. Transcriptional bursting from the HIV-1 promoter is a significant source of stochastic noise in HIV-1 gene expression. Biophys J. 2010; 98:L32–34. [PubMed: 20409455]

131. Sinnamon JR, Czaplinski K. RNA detection in situ with FISH-STICs. RNA. 2014; 20:260–66. [PubMed: 24345395]

132. Skupsky R, Burnett JC, Foley JE, Schaffer DV, Arkin AP. HIV promoter integration site primarily modulates transcriptional burst size rather than frequency. PLOS Comput Biol. 2010; 6:e1000952. [PubMed: 20941390]

133. Smith C, Lari A, Derrer CP, Ouwehand A, Rossouw A, et al. In vivo single-particle imaging of nuclear mRNA export in budding yeast demonstrates an essential role for Mex67p. J Cell Biol. 2015; 211:1121–30. [PubMed: 26694837]

134. Smith CS, Preibisch S, Joseph A, Abrahamsson S, Rieger B, et al. Nuclear accessibility of β-actin mRNA is measured by 3D single-molecule real-time tracking. J Cell Biol. 2015; 209:609–19. [PubMed: 26008747]

135. Stasevich TJ, Hayashi-Takanaka Y, Sato Y, Maehara K, Ohkawa Y, et al. Regulation of RNA polymerase II activation by histone acetylation in single living cells. Nature. 2014; 516:272–75. [PubMed: 25252976]

136. Suter DM, Molina N, Gatfield D, Schneider K, Schibler U, Naef F. Mammalian genes are transcribed with widely different bursting kinetics. Science. 2011; 332:472–74. [PubMed: 21415320]

137. Sutherland H, Bickmore WA. Transcription factories: gene expression in unions? Nat Rev Genet. 2009; 10:457–66. [PubMed: 19506577]

138. Takizawa PA, Vale RD. The myosin motor, Myo4p, binds Ash1 mRNA via the adapter protein, She3p. PNAS. 2000; 97:5273–78. [PubMed: 10792032]

139. Tanenbaum ME, Gilbert LA, Qi LS, Weissman JS, Vale RD. A protein-tagging system for signal amplification in gene expression and fluorescence imaging. Cell. 2014; 159:635–46. [PubMed: 25307933]

140. Taniguchi Y, Choi PJ, Li GW, Chen H, Babu M, et al. Quantifying *E. coli* proteome and transcriptome with single-molecule sensitivity in single cells. Science. 2010; 329:533–38. [PubMed: 20671182]

141. Torres-Padilla ME, Chambers I. Transcription factor heterogeneity in pluripotent stem cells: a stochastic advantage. Development. 2014; 141:2173–81. [PubMed: 24866112]

142. Trcek T, Chao JA, Larson DR, Park HY, Zenklusen D, et al. Single-mRNA counting using fluorescent in situ hybridization in budding yeast. Nat Protoc. 2012; 7:408–19. [PubMed: 22301778]

143. Trcek T, Grosch M, York A, Shroff H, Lionnet T, Lehmann R. *Drosophila* germ granules are structured and contain homotypic mRNA clusters. Nat Commun. 2015; 6:7962. [PubMed: 26242323]

144. Trcek T, Larson DR, Moldon A, Query CC, Singer RH. Single-molecule mRNA decay measurements reveal promoter-regulated mRNA stability in yeast. Cell. 2011; 147:1484–97. [PubMed: 22196726]

145. Van Keymeulen A, Blanpain C. Tracing epithelial stem cells during development, homeostasis, and repair. J Cell Biol. 2012; 197:575–84. [PubMed: 22641343]

146. Vargas DY, Shah K, Batish M, Levandoski M, Sinha S, et al. Single-molecule imaging of transcriptionally coupled and uncoupled splicing. Cell. 2011; 147:1054–65. [PubMed: 22118462]

147. Vera M, Pani B, Griffiths LA, Muchardt C, Abbott CM, et al. The translation elongation factor eEF1A1 couples transcription to translation during heat shock response. eLife. 2014; 3:e03164. [PubMed: 25233275]

148. Vinuelas J, Kaneko G, Coulon A, Vallin E, Morin V, et al. Quantifying the contribution of chromatin dynamics to stochastic gene expression reveals long, locus-dependent periods between transcriptional bursts. BMC Biol. 2013; 11:15. [PubMed: 23442824]

149. Viswanathan S, Williams ME, Bloss EB, Stasevich TJ, Speer CM, et al. High-performance probes for light and electron microscopy. Nat Methods. 2015; 12:568–76. [PubMed: 25915120]

150. Wang C, Han B, Zhou R, Zhuang X. Real-time imaging of translation on single mRNA transcripts in live cells. Cell. 2016; 165:990–1001. [PubMed: 27153499]

151. Weill L, Belloc E, Bava FA, Mendez R. Translational control by changes in poly(A) tail length: recycling mRNAs. Nat Struct Mol Biol. 2012; 19:577–85. [PubMed: 22664985]

152. Williamson I, Berlivet S, Eskeland R, Boyle S, Illingworth RS, et al. Spatial genome organization: contrasting views from chromosome conformation capture and fluorescence in situ hybridization. Genes Dev. 2014; 28:2778–91. [PubMed: 25512564]

153. Woringer M, Darzacq X, Izeddin I. Geometry of the nucleus: a perspective on gene expression regulation. Curr Opin Chem Biol. 2014; 20:112–19. [PubMed: 24981829]

154. Wu B, Buxbaum AR, Katz ZB, Yoon YJ, Singer RH. Quantifying protein-mRNA interactions in single live cells. Cell. 2015; 162:211–20. [PubMed: 26140598]

155. Wu B, Eliscovich C, Yoon Y, Singer RH. Translation dynamics of single mRNAs in live cells and neurons. Science. 2016; 352:1430–35. [PubMed: 27313041]

156. Xu H, Sepulveda LA, Figard L, Sokac AM, Golding I. Combining protein and mRNA quantification to decipher transcriptional regulation. Nat Methods. 2015; 12:739–42. [PubMed: 26098021]

157. Yan X, Hoek TA, Vale RD, Tanenbaum ME. Dynamics of translation of single mRNA molecules in vivo. Cell. 2016; 165:976–89. [PubMed: 27153498]

158. Zeisel A, Munoz-Manchado AB, Codeluppi S, Lonnerberg P, La Manno G, et al. Brain structure. Cell types in the mouse cortex and hippocampus revealed by single-cell RNA-seq. Science. 2015; 347:1138–42. [PubMed: 25700174]

159. Zenklusen D, Larson DR, Singer RH. Single-RNA counting reveals alternative modes of gene expression in yeast. Nat Struct Mol Biol. 2008; 15:1263–71. [PubMed: 19011635]

160. Zid BM, O'Shea EK. Promoter sequences direct cytoplasmic localization and translation of mRNAs during starvation in yeast. Nature. 2014; 514:117–21. [PubMed: 25119046]
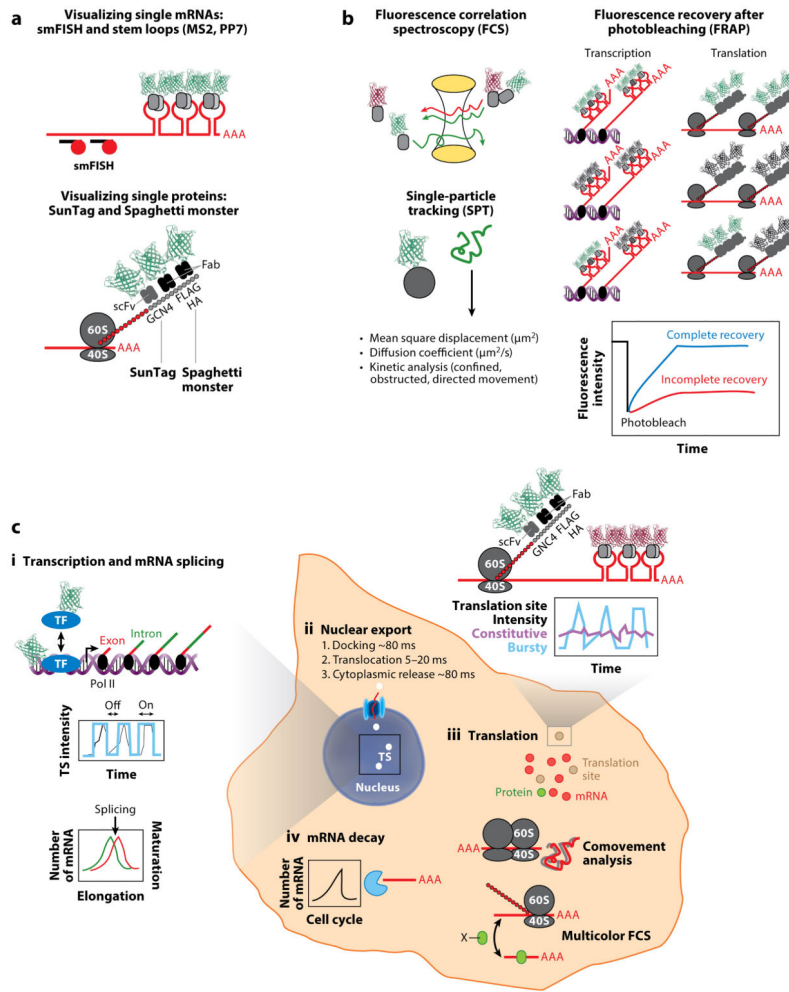
Vera M, et al. 2016.
Annu. Rev. Genet. 50:267–91

Figure 1.
Single-cell and single-molecule imaging technologies to analyze gene expression regulation. (*a*) Tools to achieve single-molecule resolution in cells. Visualizing single mRNA: schematic of an mRNA molecule with repetitions of MS2 or PP7 stem-loops genetically inserted in the 3′ untranslated region (3′ UTR). Tandem dimers of MCP (MS2 capsid protein) or PCP (PP7 capsid protein) (*gray circles*) fused to two molecules of green fluorescent protein (GFP) (*green crystal structure*) bind to each loop to label mRNAs with two GFP molecules per stem-loop in live cells. Multiple smFISH (single-molecule fluorescence in situ hybridization) probes labeled with a fluorophore bind to their complementary sequence in the mRNA, allowing detection of single mRNA molecules in fixed cells. Visualization of single proteins: schematic of a translating mRNA genetically modified with multiple GCN4 epitopes (SunTag) or Flag and HA epitopes (Spaghetti monster) sequences. As GCN4 or Flag and HA sequences are translated, they are recognized by scFv (SunTag) or Fab (Spaghetti monster) antibodies fused to GFP. Each protein is labeled with multiple GFP molecules at its N terminus. (*b*) Techniques to analyze single-molecule interactions and dynamics in live cells. Fluorescence correlation spectroscopy (FCS) uses a focused laser to

excite fluorescently tagged molecules as they pass through the femtoliter volume. On the basis of the brightness correlation between two spectrally different fluorophores, their molecular interaction is inferred. Single-particle tracking (SPT) follows molecules from frame to frame, allowing the indicated measurements. Fluorescence recovery after photobleaching (FRAP) measures the rate of fluorescence intensity recovery and can be used to determine the kinetics of transcription and translation. In the case of transcription (*left panel*), mRNAs are tagged in the 5′ UTR with the MS2-MCP system, and in the case of translation (*right panel*), the proteins are tagged at the N terminus with the SunTag system. The plot represents measurements of fluorescence intensity before and over time after photobleaching, which can be used to calculate the mRNA or protein synthesis rate. (*c*) Schematic of a eukaryotic cell to illustrate how each step of gene expression is studied at the single-molecule level (starting from the *top left* and *moving clockwise*). (*i*) Transcription and mRNA splicing. The residence time of a fluorescently labeled transcription factor (TF) on DNA can be quantified using super-resolution and SPT techniques. By labeling nascent transcripts, the fluorescence intensity of the transcription site (TS) can be monitored over time to define the frequency, intensity, and amplitude of transcription. Cotranscriptional splicing can be visualized by labeling exons and introns on a nascent mRNA with spectrally different fluorophores. A plot of different probes' intensities allows us to measure the number of mRNAs per TS, calculate the transcription elongation rate, and visualize mRNA splicing. (*ii*) Nuclear export. SPT of single mRNAs as they exit the nucleus indicates three distinct stages of nuclear export through the nuclear pore complex. (*iii*) Translation. Simultaneous imaging of mRNAs and proteins (*red* and *green dots*, respectively) reveals the dynamics of translation. Magnification of a site of translation (*orange dot* indicates the colocalization and comovement of an mRNA and more than one peptide). Magnification shows a schematic of a translating transcript genetically modified with the MS2-MCP [bound to red fluorescent protein (RFP)] system in the 3′ UTR and the SunTag system (scFv or Spaghetti monster bound to GFP) at the N terminus. A plot of the protein signal (GFP) describes the dynamics of translation. Labeling of mRNAs and ribosomes or RNA-binding proteins and comovement analysis or FCS reveals the dynamics of polysomes and the interaction of mRNA-binding proteins with mRNAs. (*iv*) mRNA decay. Correlation of the number of mRNAs with the cell cycle reveals a time-dependent switch in the mRNA's half-life.
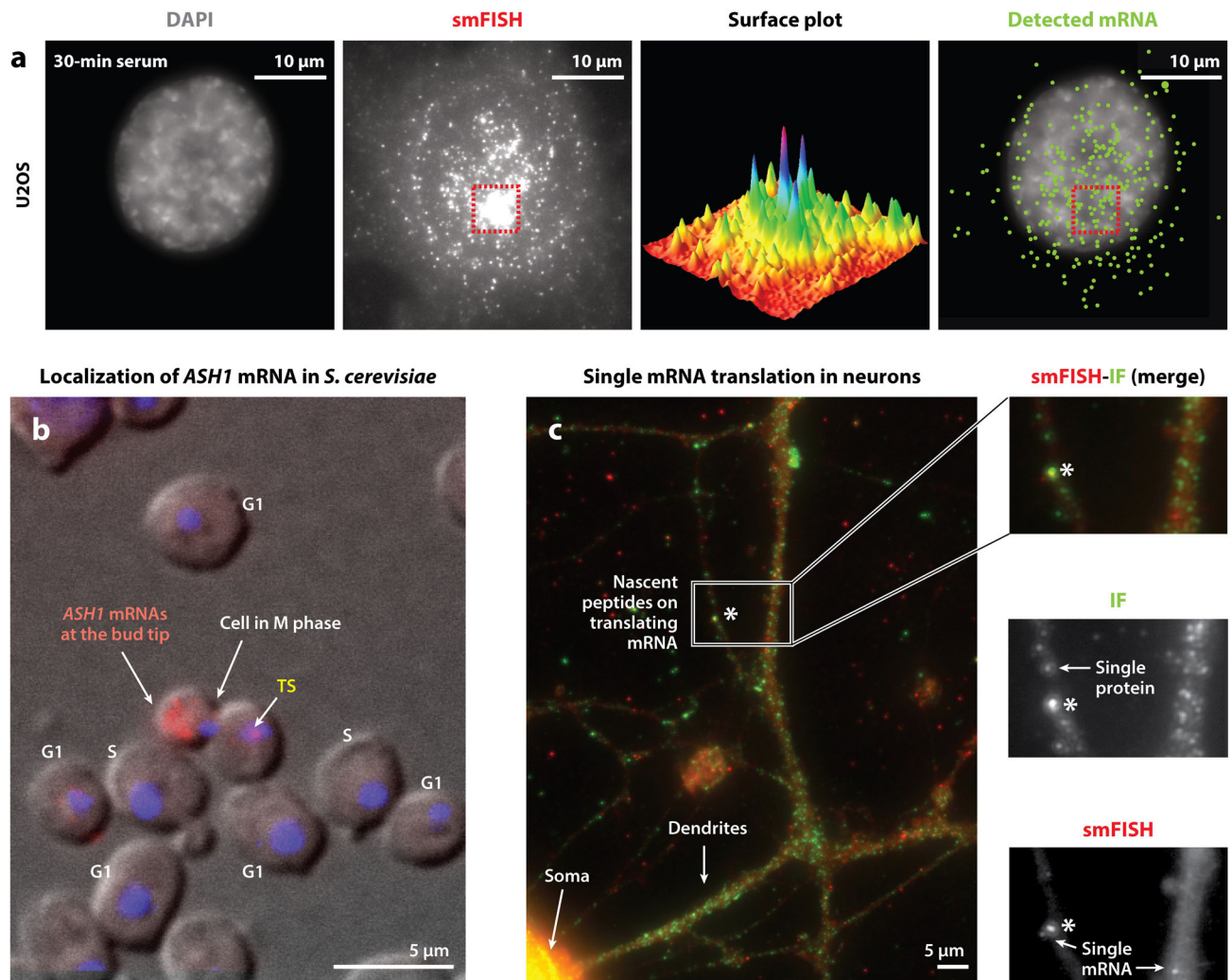
Figure 2.

Examples of single-cell and single-molecule analysis of transcription, mRNA localization, and translation. (*a*) smFISH (single-molecule fluorescence in situ hybridization) for the *c-Fos* gene in a U2OS cell at 30 min after serum induction. The signal in proximity of the transcription site (TS) appears saturated because of scaling to show individual mature mRNAs. The surface plot (not to scale) shows the area indicated with a red dashed line. Detected mature mRNAs are shown as green spots on top of the DAPI image. Panel *a* adapted from Senecal et al. (123). (*b*) Specific expression and localization of *ASH1* mRNA in *Saccharomyces cerevisiae*. The representative image shows smFISH of *ASH1* (*red signal*) in fixed cells in an asynchronous population (different stages of the cell cycle are indicated in *white*). The *ASH1* gene is exclusively expressed during anaphase of mitosis (M phase). *ASH1* transcripts (*red signal*) localize at the bud tip and are degraded before G1, the next stage of the cell cycle. Nuclei stained with DAPI are shown in blue. This unpublished image

was kindly provided by Evelina Tutucci. (*c*) Translation sites in neurons visualized by an smFISH-immunofluorescence (IF) experiment on hippocampal neurons. The three boxes on the far right are magnifications of the same area. IF (*green*) recognizes the scFv-sfGFP bound to the 24 copies of the GCN4 sequence (SunTag system). smFISH (*red*) recognizes the transcript coding for the GCN4 polypeptide. The asterisk indicates a single mRNA translating several nascent peptides. The translation site is more intense than single proteins because several nascent peptides are being synthesized from the same single mRNA. This unpublished image was kindly provided by Carolina Eliscovich.

Table 1

Imaging techniques commonly used for single-cell and single-molecule studies of gene regulation[a]

Microscopy tools	Concepts and capabilities
Photoactivated localization microscopy (PALM)/stochastic optical reconstruction microscopy (STORM)	Photoswitchable fluorophores are used to localize single molecules with a precision of ~20 nm
Structured illumination microscopy (SIM)	Interference (moiré effect) between the structured illumination pattern and the structure of the object is used to improve the optical resolution to ~100 nm
Multifocus microscopy (MFM)	A multifocus grating is used to acquire images of several focal planes in a single shot, facilitating high-speed 3D imaging
Light sheet microscopy (LSM)	A thin laser light sheet is used to illuminate the sample perpendicularly to the detection axis for good optical sectioning, fast 3D scanning, and minimal photobleaching and phototoxicity
Two-photon microscopy (TPM)	Two-photon absorption of near-infrared light is used to image live tissues down to a depth of ~1 mm with minimal photobleaching out of the focal volume
Analysis tools	**Concepts and capabilities**
Single-particle tracking (SPT)	Individual molecules are localized in each frame and tracked over time with high spatial resolution below the diffraction limit
Fluorescence recovery after photobleaching (FRAP)	A region of interest is photobleached and then recovery of fluorescence is recorded over time to measure the fraction and diffusion coefficient of mobile molecules
Fluorescence correlation spectroscopy (FCS)/fluorescence fluctuation spectroscopy (FFS)	Fluctuation in fluorescence signal is used to measure the diffusion coefficient, concentration, and molecular interactions. Heterospecies partition (HSP) analysis can be used to extract the binding curves and stoichiometry for protein-protein and protein-RNA interactions
FISH-QUANT	This MATLAB-based software can be used to count the number of nascent mRNAs per active transcription site (TS) by comparing the TS signal with the average intensity of individual mature mRNAs
Hidden Markov modeling (HMM)-Bayes analysis (100)	This MATLAB-based software uses Bayesian model selection and hidden Markov modeling to infer stochastic switching between active transport and diffusive motion of a particle

[a]The quantification of TF mobility could diverge because of the artifacts caused by FRAP, FCS, and SPT (54). However, three approaches yielded similar estimates for both the fraction of p53 molecules bound to chromatin (only about 20%) and the residence time of these bound molecules (≈1.8 s) (99).